Article

Micromagnetic Analysis of Monolayer L10-FePt and Bilayer L10-FePt/Fe Ultrathin Films

Nikolaos Maniotis * and Evangelos Papaioannou

Posted Date: 17 November 2025

doi: 10.20944/preprints202511.1187.v1

Keywords: micromagnetic simulation; $L1_0$ FePt ultrathin films; FePt/Fe thin films; hysteresis loop; exchange-spring magnet; exchange correlation length; magnetic anisotropy

 doi:10.20944/preprints202511.1187.v1

Article

Micromagnetic Analysis of Monolayer L10-FePt and Bilayer L10-FePt/Fe Ultrathin Films

Nikolaos Maniotis * and Evangelos Th. Papaioannou

Department of Physics, Aristotle University of Thessaloniki, 54124 Thessaloniki, Greece

* Correspondence: nimaniot@physics.auth.gr

Abstract

This work presents a micromagnetic investigation of monolayer $L1_0$ FePt and FePt/Fe bilayer thin films to clarify the role of thickness, composition, and exchange coupling in their magnetic behavior. Simulations were performed using the Landau–Lifshitz–Gilbert formalism implemented in *OOMMF*, with realistic material parameters and geometries. For FePt monolayers, film thicknesses of 1–20 nm were examined, revealing a non-monotonic coercivity trend: the coercive field increased from 35 mT at 1 nm to 136 mT at 10 nm and decreased to 69 mT at 20 nm. This evolution indicates a transition from localized reversal to domain-wall–mediated switching once the film exceeds the exchange length (10–20 nm). Additional simulations varying Fe concentration (48–68%) through the exchange stiffness constant showed that higher Fe content strengthens magnetic coupling and increases coercivity. Bilayer systems combining a 2 nm FePt layer with Fe layers of 10 and 12 nm exhibited rectangular, saturated loops, confirming strong exchange coupling and exchange-spring behavior. The results identify 2 nm FePt as the optimal thickness for achieving full saturation, balanced coercivity, and thermal stability in FePt/Fe thin-film architectures.

Keywords: micromagnetic simulation; $L1_0$ FePt ultrathin films; FePt/Fe thin films; hysteresis loop; exchange-spring magnet; exchange correlation length; magnetic anisotropy

1. Introduction

Magnetic nanostructures and thin films with tailored magnetic properties are central to the development of next-generation spintronic devices, high-density magnetic recording media, and permanent magnets [1–3]. Among these materials, chemically ordered $L1_0$ FePt alloys have attracted considerable attention due to their exceptionally high magnetocrystalline anisotropy (≈7 × 10^6 J/m^3), thermal stability, and large coercivity [4,5]. These characteristics make FePt an excellent candidate for hard magnetic layers in composite systems, particularly in exchange-coupled bilayers and multilayer heterostructures [6–8].

The concept of the exchange-spring magnet, originally proposed to combine the high coercivity of a hard phase with the high magnetization of a soft phase, provides a pathway to achieving superior magnetic performance [9–11]. In such systems, the interfacial exchange interaction allows the magnetization to gradually rotate from the hard to the soft layer under an external magnetic field, mimicking the elastic behavior of a mechanical spring [12]. The degree of coupling, and hence the magnetization reversal mechanism, strongly depends on the relative thickness and anisotropy of the two magnetic components [13,14]. A balance between interfacial exchange strength and individual layer thickness is therefore essential for optimizing both coercivity and saturation magnetization.

While many experimental and theoretical studies have explored FePt-based bilayers [15–17], the specific influence of FePt layer thickness at the monolayer and ultrathin limit on magnetic hysteresis and saturation behavior remains less understood. Previous work has indicated that excessive FePt thickness leads to rigid magnetic coupling, preventing full magnetization reversal at moderate fields [18], whereas too thin a hard layer can result in thermal instability and reduced anisotropy [19]. Thus,

 doi:10.20944/preprints202511.1187.v1

identifying an optimal FePt thickness that enables exchange-spring behavior under practical magnetic field strengths is crucial for both fundamental understanding and technological application.

In this study, we perform micromagnetic simulations to systematically investigate the effect of FePt thickness on the magnetic hysteresis of monolayer FePt and bilayer FePt/Fe systems under an applied field of 500 mT. FePt layers of 1, 2, 5, and 10 nm were modeled to assess their coercivity and saturation response. The 2 nm FePt film was identified as the most favorable configuration, reaching full saturation while maintaining moderate coercivity. When combined with Fe layers of 10 and 12 nm, the resulting FePt/Fe bilayers achieved complete magnetization reversal, demonstrating a clear transition from a rigidly coupled system to an exchange-spring configuration as FePt thickness decreased. From a thermodynamic viewpoint, 1 nm FePt films exhibit instability, reinforcing the 2 nm thickness as the optimum for achieving stable and efficient exchange-spring magnet behavior. To further extend this analysis, additional simulations were carried out for a 20 nm $L1_0$ FePt monolayer and for alloys with varying Fe concentrations, indirectly tuned through the exchange stiffness constant. The 20 nm FePt film exhibited a smoother hysteresis loop and a lower coercive field compared to the 5 and 10 nm cases, consistent with magnetization reversal occurring over distances comparable to or exceeding the exchange length (10–20 nm for Fe-based systems). This behavior confirms the transition from localized, nucleation-dominated reversal in thinner layers to domain-wall–mediated switching in thicker ones. Moreover, increasing Fe concentration from 48% to 68% enhanced exchange coupling and slightly increased coercivity, with the lowest Fe content yielding full saturation and reduced noise in the loop. These findings provide additional insight into the interplay between exchange stiffness, layer thickness, and composition in determining the reversal mechanisms and stability of FePt-based magnetic thin films.

2. Materials and Methods

Micromagnetic simulations were performed by numerically solving the standard Landau–Lifshitz–Gilbert (LLG) equation [20] to model the dynamic evolution of magnetization under an applied magnetic field. The simulations were implemented using the Object Oriented MicroMagnetic Framework (OOMMF), which provides a finite-difference solution of the LLG equation over a discretized magnetic structure [21].

The computational model consisted of a single $L1_0$ FePt layer (monolayer case) and a bilayer configuration composed of FePt and Fe films. In the bilayer geometry, two atlas boxes were defined in OOMMF: one labeled *bottom* (corresponding to the FePt hard layer) and one labeled *top* (corresponding to the Fe soft layer). The interfacial region was explicitly defined to include the exchange interaction between the two materials, ensuring continuous magnetization coupling across the interface.

The system was discretized using a fine rectangular mesh, which provided a good balance between numerical accuracy and computational efficiency. The external in-plane magnetic field was applied along a random orientation compared to the easy axis of FePt, and the hysteresis loops were obtained by gradually sweeping the field from positive to negative saturation up to 500 mT.

The material parameters were selected from typical experimental and theoretical values reported for bulk and thin-film Fe and $L1_0$ FePt systems [22,23]. The saturation magnetization was set to $M_{Fe} = 1.2 \times 10^6$ A/m and $M_{FePt} = 0.5 \times 10^6$ A/m while exchange stiffness constants were assigned as $A_{FePt} = 1.2 \times 10^{-11}$ J/m, $A_{Fe} = 2.8 \times 10^{-11}$ J/m and $A_{ex} = 1.8 \times 10^{-11}$ J/m. The latter constant is referred to the interface exchange coupled constant. For the magnetocrystalline anisotropy, the following literature values were used: $K_{Fe} = 4.8 \times 10^4$ J/m^3 and $K_{FePt} = 6 \times 10^6$ J/m^3. For the simulations, the magnetic anisotropy orientation was chosen based on typical thin-film growth behavior. The $L1_0$ FePt layer was assigned a perpendicular (out-of-plane) uniaxial anisotropy along the c-axis, which is commonly observed in sputtered or annealed FePt films. The Fe layer, being magnetically soft with very low intrinsic anisotropy, was assumed to be in-plane isotropic, with its magnetization free to align along the applied field or follow exchange coupling with the FePt layer. Hysteresis loops were simulated for both in-plane and out-of-plane applied field orientations to capture the directional

 doi:10.20944/preprints202511.1187.v1

dependence of magnetization reversal and to evaluate the effect of perpendicular anisotropy in the bilayer systems.

The hysteresis behavior was calculated by applying an external magnetic field from +500 mT to −500 mT, using quasi-static relaxation at each field step to ensure equilibrium magnetization states. Magnetization reversal processes were analyzed by recording the average magnetization, coercivity, and saturation field for each FePt thickness (1, 2, 5, and 10 nm) and for FePt/Fe bilayers with Fe layers of 10 and 12 nm. Temperature was set at room temperature 300 K and a damping coefficient of 0.1 was also utilized. The time step was equal to 2.5×10^{-12} seconds.

3. Results

3.1. Monolayer

In Figure 1 the simulated hysteresis loops are presented for monolayer $L1_0$ FePt films with thicknesses of (a) 1 nm, (b) 2 nm, (c) 5 nm, and (d) 10 nm, obtained under an applied magnetic field of ±500 mT. The evolution of loop shape with increasing thickness reflects changes in coercivity, anisotropy, and the ability of the magnetization to reach saturation within the applied field range. For the 1 nm FePt film (Figure 1a), the hysteresis loop is narrow, indicating low coercivity and incomplete magnetic ordering. Such behavior is typical for ultrathin FePt layers where surface and interface effects dominate, reducing effective anisotropy and making the magnetization thermally unstable. At 2 nm thickness (Figure 1b), the loop becomes noticeably more vertical in the central region, indicating a sharper magnetization reversal and stronger anisotropic response. The magnetization approaches full saturation within the applied field range, suggesting that the anisotropy and exchange stiffness are sufficient to stabilize a coherent reversal process while maintaining good field response. Although the coercivity is lower than in thicker films, this configuration provides the best balance between switching sharpness and saturation behavior. For 5 nm and 10 nm FePt layers (Figures 1c and 1d), the hysteresis loops broaden and exhibit gradual, unsaturated magnetization curves, even at ±500 mT.

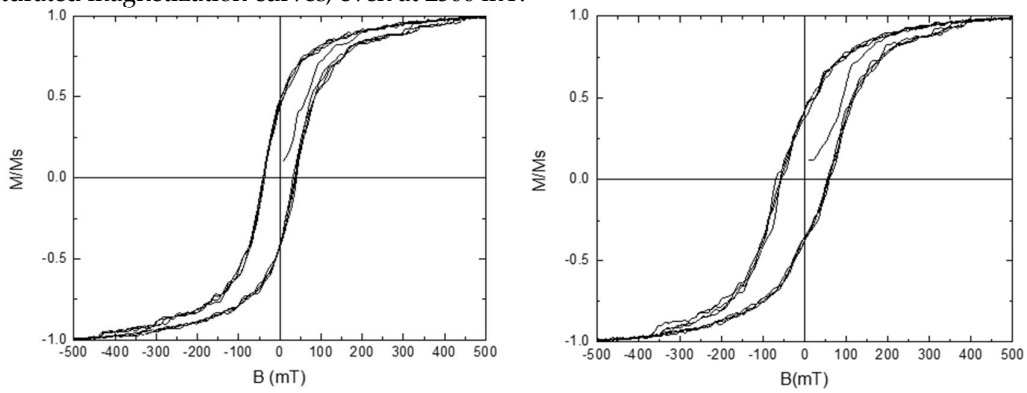

(**a**) (**b**)

 doi:10.20944/preprints202511.1187.v1

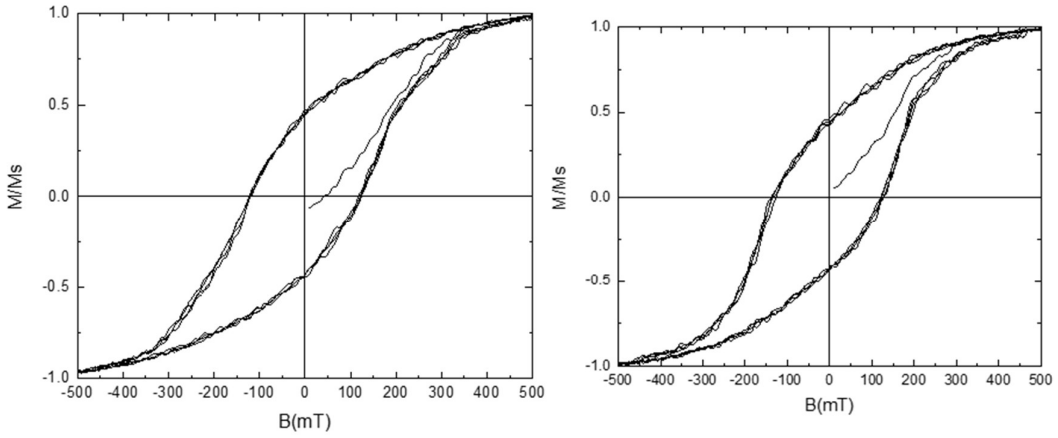

(**c**) (**d**)

Figure 1. Simulated hysteresis loops of monolayer $L1_0$ FePt thin films with different thicknesses: (**a**) 1 nm, (**b**) 2 nm, (**c**) 5 nm, and (**d**) 10 nm. The applied magnetic field range was ±500 mT. The magnetization values are normalized to the saturation magnetization value. The 2 nm film exhibits a more vertical loop shape, indicating a sharper magnetization reversal and near-saturation behavior, while thicker films (5 nm and 10 nm) display more gradual, unsaturated magnetization curves due to strong anisotropy and exchange stiffness.

This incomplete reversal reflects the strong magnetocrystalline anisotropy and exchange stiffness of thicker FePt films, which prevent full alignment of magnetic moments at moderate fields. These films behave as stiff magnets, requiring substantially higher fields for complete magnetization reversal. Overall, the simulation results indicate that the 2 nm FePt layer provides the optimum thickness, achieving a near-saturated state at 500 mT with a sharper magnetization transition. Thinner films (1 nm) are unstable, whereas thicker films (≥5 nm) remain partially unsaturated under the same conditions due to their increased anisotropy and exchange. Note here that this size has alredy been utilized as optimum in previous experimental study in THz emission from Fe/Pt spintronic emitters with L10-FePt alloyed interface [24].

3.2. Bilayer

To further explore the effect of soft–hard magnetic coupling, bilayer systems composed of a 2 nm $L1_0$ FePt layer and Fe soft layers of 10 nm and 12 nm thickness were simulated. Figure 2 shows the resulting hysteresis loops for these two bilayer configurations. In both cases, the loops are narrow, rectangular, and fully saturated within the applied magnetic field range of ±500 mT. This behavior contrasts sharply with the monolayer FePt films of larger thickness (5 and 10 nm), where strong anisotropy prevente complete magnetization reversal under the same field conditions. The addition of the soft Fe layer markedly enhances the magnetic response, enabling coherent rotation of magnetization throughout the structure. The observed saturation arises from two key factors: (i) the presence of the soft Fe phase, which facilitates magnetization reversal through exchange coupling with the FePt layer; and (ii) the optimized thickness of the FePt layer (2 nm), which ensures sufficient anisotropy for magnetic stability while maintaining effective exchange communication across the interface. The interfacial exchange stiffness defined in the model ($A_{ex} = 1.8 \times 10^{-11}\, J/m$) enables a gradual yet complete rotation of the spins, leading to a single-step reversal and a nearly rectangular hysteresis loop. The results confirm that the FePt/Fe bilayer behaves as an exchange-spring magnet, where the hard FePt layer provides the anisotropy and coercivity, while the soft Fe layer contributes to rapid saturation and enhanced remanence. Increasing the Fe layer thickness from 10 nm to 12 nm does not significantly alter the overall shape of the loop, indicating that the exchange coupling remains strong across this thickness range.

 doi:10.20944/preprints202511.1187.v1

On the whole, the bilayer configuration effectively transforms the system from a rigid single-phase magnet (as in thicker FePt monolayers) to a compliant exchange-spring structure, capable of reaching full saturation at moderate fields.

To further investigate the anisotropic behavior of the optimized bilayer configuration, additional simulations were performed for the out-of-plane magnetic field orientation in the FePt(2 nm)/Fe(10 nm) system. The corresponding hysteresis loop is presented in the inset of Figure 2. In contrast to the in-plane results, which exhibited rectangular and fully saturated loops, the out-of-plane direction produced a non-rectangular hysteresis loop with significantly lower squareness and higher coercivity. Specifically, the ratio of remanent to saturation magnetization (M_r/M_s) was approximately 36%, indicating that the magnetization does not retain a large remanent component once the external field is removed. This reduction in squareness reflects the competition between the strong in-plane exchange coupling within the Fe layer and the perpendicular anisotropy contribution from the FePt hard layer. The increased coercivity observed in the out-of-plane configuration suggests that the system requires a higher field to overcome the anisotropy barrier when magnetization is forced to deviate from its preferred in-plane alignment. This behavior is consistent with the expected uniaxial anisotropy of $L1_0$ FePt, whose easy axis is oriented perpendicular to the film plane. The coupling between the FePt and Fe layers thus gives rise to a composite anisotropy, where the soft Fe layer promotes in-plane rotation, while the FePt layer preserves a strong perpendicular tendency. Generally, the difference between the in-plane and out-of-plane loops confirms that the FePt/Fe bilayers possess a well-defined perpendicular uniaxial anisotropy, combined with excellent in-plane switching performance. This anisotropic behavior could be advantageous for applications requiring tunable magnetization directions, such as perpendicular magnetic recording or spintronic multilayer architectures.

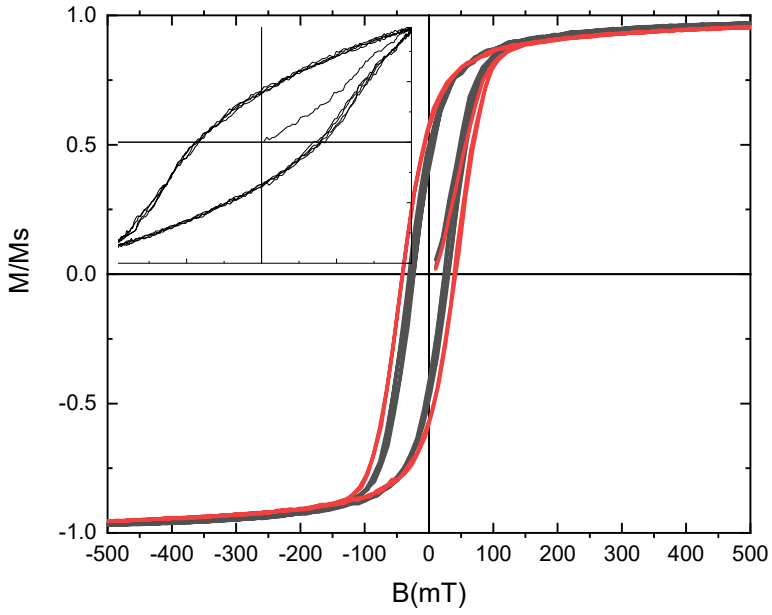

Figure 2. Simulated hysteresis loops of FePt/Fe bilayers with a 2 nm $L1_0$ FePt hard layer and soft Fe layers of different thicknesses. The black colored loop corresponds to FePt(2 nm)/Fe(10 nm) film while the red colored loop to the FePt(2 nm)/Fe(12 nm). Both bilayers exhibit narrow, rectangular loops and complete saturation within ±500 mT, demonstrating efficient exchange coupling between the hard and soft layers. The soft Fe phase promotes easy magnetization reversal, while the FePt layer maintains coercivity and thermal stability. **Inset:** Out-of-plane hysteresis loop of the FePt(2 nm)/Fe(10 nm) bilayer. Unlike the in-plane configuration, the loop exhibits a non-rectangular shape with reduced squareness ($M_r/M_s \approx 0.36$) and higher coercivity. This behavior

 doi:10.20944/preprints202511.1187.v1

indicates the presence of strong perpendicular uniaxial anisotropy arising from the $L1_0$ FePt layer and the combined anisotropic coupling within the bilayer structure.

4. Discussion

The hysteresis loops for FePt monolayers up to 10 nm thickness show pronounced irregularities (abrupt jumps) during magnetization reversal, whereas films thicker than ≈10 nm (we will show subsequently the 20 nm case for different Fe concentrations) display considerably smoother loops and a reduced coercivity that approaches the value observed for the 2 nm film. This systematic change in reversal character can be interpreted in terms of the characteristic exchange length and the dominant reversal mode of the films. The exchange length, L_{ex}, is the characteristic length scale over which exchange energy enforces local uniformity of the magnetization. When structural dimensions (film thickness, domain-wall width, or inhomogeneity size) are of the same order as or smaller than L_{ex}, exchange coupling strongly constrains spatial variations of the magnetization and reversal tends to be non-uniform and localized. Conversely, when the film thickness exceeds L_{ex}, the system can support more extended domain structures and domain-wall motion becomes the dominant reversal mechanism. In thin films, the exchange length is $L_{ex} = (A/K_m)^{1/2}$, where A is the exchange stiffness constant and K_m is a magnetostatic energy density, $K_m = {}^1/_2\mu_0 M_s^2$ (SI) or $2\pi M_s^2$ (cgs emu) [25].

Using the material parameters employed in our simulations ($A_{Fe} = 2.8 \times 10^{-11}$ J·m^{-1}, $M_{s,Fe} = 1.2 \times 10^6$ A·m^{-1}; $A_{FePt} = 1.2 \times 10^{-11}$ J·m^{-1}, $M_{s,FePt} = 0.5 \times 10^6$ A·m^{-1}, : $K_{Fe} = 4.8 \times 10^4$ J/m^3 and $K_{FePt} = 6 \times 10^6$ J/m^3), the exchange lengths evaluate to approximately $L_{ex}^{Fe} \approx 5.6$ nm, and $L_{ex}^{FePt} \approx 8.7$ nm. For Fe-based alloys, the typical values of L_{ex} lie in the range of 10 – 20 nm [26,27]. Therefore, both amorphous and nanocrystalline alloys fall under the regime if their thickness is lower than L_{ex}.

The evolution of hysteresis loops with film thickness and Fe concentration can be understood in terms of the exchange length and the corresponding magnetization reversal mechanisms. When the FePt film thickness is comparable to, or smaller than, the characteristic exchange length (L_{ex}), the exchange interaction strongly constrains local variations of magnetization, leading to nonuniform and localized reversal processes. Under these conditions, magnetization switching proceeds through discrete nucleation and depinning events, which appear as abrupt jumps or noise in the simulated hysteresis loops. This behavior was clearly observed in films up to 10 nm, where the effective magnetic coupling is strong and reversal is dominated by local nucleation rather than by domain-wall propagation. The high coercivity in this range arises from the large anisotropy energy barriers that must be overcome during each localized switching event.

When the film thickness exceeds approximately 10 nm, as in the 20 nm samples, the system becomes thicker than the effective exchange length. In this regime, the magnetization can vary more smoothly across the thickness, allowing the formation and propagation of extended domain walls. Consequently, the magnetization reversal becomes collective, the hysteresis loops appear smoother, and the coercivity decreases. This transition marks the crossover from exchange-dominated localized reversal to domain-wall–mediated switching, consistent with typical exchange lengths reported for Fe-based alloys ($L_{ex} \approx 10$–20 nm).

To evaluate how the Fe concentration influences the overall magnetic behavior, three compositions were simulated by adjusting the exchange stiffness constant (A), which effectively represents the variation in Fe content within the FePt/Fe alloy system. Based on literature data [28], $A = 13$ pJ/m corresponds to approximately 68% Fe, $A = 12$ pJ/m to 60% Fe, and $A = 11$ pJ/m to 48% Fe.

As shown in Figure 3, all three 20 nm films exhibit smooth and nearly rectangular hysteresis loops, with no abrupt jumps or noise as observed in thinner samples (≤ 10 nm). The disappearance of discontinuities further confirms that the film thickness exceeds the effective exchange length, allowing the magnetization to reverse through collective domain-wall motion rather than localized switching.

 doi:10.20944/preprints202511.1187.v1

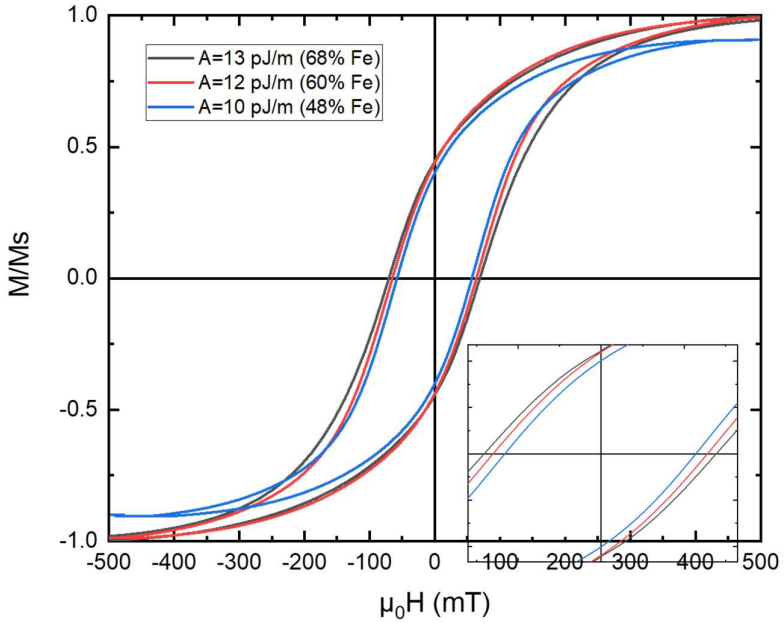

Figure 3. Simulated hysteresis loops of 20 nm FePt monolayer films for different Fe concentrations. The Fe concentration was indirectly introduced through the exchange stiffness constant A: 13 pJ/m (≈ 68% Fe), 12 pJ/m (≈ 60% Fe), and 11 pJ/m (≈ 48% Fe). All films exhibit smooth, saturated loops, confirming the transition to domain-wall–mediated reversal when the thickness exceeds the exchange length. The 48% Fe film shows the lowest coercivity and complete saturation, whereas higher Fe concentrations yield slightly higher coercivity and remanence due to stronger exchange coupling. The inset shows the minor loop (magnification of the major loop at the vicinity of lower magnetic field amplitude) at ±80 mT where the difference in coercivity between the three different concentrations is evident.

A moderate dependence of coercivity and squareness on Fe content is observed. The 48% Fe composition (A = 11 pJ/m) displays the lowest coercivity and achieves full saturation, consistent with a slightly weaker exchange stiffness that promotes easier domain-wall propagation. In contrast, the 60% and 68% Fe compositions (A = 12–13 pJ/m) exhibit slightly higher coercivity and a marginally larger remanent-to-saturation ratio (M_r/M_s), indicating stronger exchange coupling and enhanced magnetic hardness. These trends reflect the direct role of the exchange stiffness in controlling the balance between coercivity and saturation: as A increases with Fe concentration, the system transitions toward a more dynamical magnetic configuration.

The non-monotonic behavior of hysteresis loop is illustrated in Figure 4 where the dependence of film thickness on coercive field Hc is depicted. The coercivity initially increases sharply from 35 mT at 1 nm to 136 mT at 10 nm, indicating the progressive dominance of the hard magnetic phase as its volume fraction grows. However, when the thickness is further increased to 20 nm, the coercivity decreases to 69 mT, reflecting a transition to a regime where magnetization reversal proceeds primarily through domain-wall motion rather than localized nucleation. This non-monotonic dependence demonstrates the well-known competing effects of anisotropy and exchange coupling [29–32]: thin films below the exchange length are strongly exchange-dominated and magnetically soft, while thicker films exceed the exchange length, allowing smoother and more collective reversal. The maximum coercivity observed around 10 nm thus marks the crossover between localized and extended reversal modes in the FePt films.

 doi:10.20944/preprints202511.1187.v1

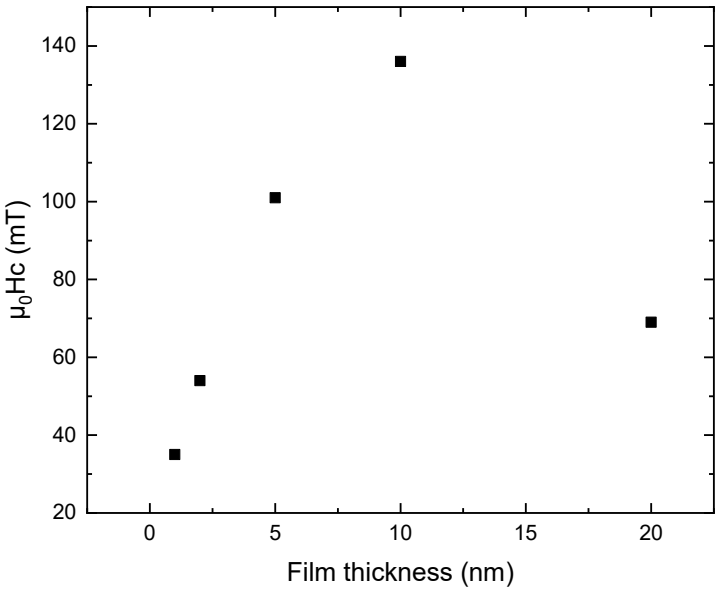

Figure 4. Dependence of coercivity on FePt-L10 layer thickness obtained from micromagnetic simulations. The coercivity increases from 35 mT at 1 nm to a maximum of 136 mT at 10 nm, followed by a marked decrease to 69 mT at 20 nm (for the highest iron concentration). This non-monotonic behavior reflects the transition from localized magnetization reversal at low thicknesses to domain-wall–mediated reversal when the film thickness exceeds the effective exchange length. The maximum near 10 nm represents the crossover between exchange-dominated and extended reversal regimes in the FePt. This behavior confirms the transition from exchange-dominated reversal at small dimensions to domain-wall–mediated magnetization switching once the total thickness exceeds the exchange length. The observed maximum around 10 nm marks the crossover between these two regimes, providing further evidence of the critical role played by exchange coupling and anisotropy balance in determining the switching behavior of FePt monolayers.

It is clear that the dependence of the loop shape on Fe concentration further supports this interpretation. In the simulations, the Fe content was introduced indirectly through the exchange stiffness constant, following literature correlations: $A = 13$pJ/m for ≈ 68% Fe, $A = 12$pJ/m for ≈ 60% Fe, and $A = 11$pJ/m for ≈ 48% Fe. Increasing Fe concentration enhances the exchange stiffness and slightly increases coercivity and squareness, indicating stronger magnetic coupling and reversibility. Conversely, the 48% Fe sample, with lower A, shows complete saturation and the lowest coercivity, consistent with easier domain-wall motion. This compositional dependence demonstrates that tuning the exchange stiffness offers a practical means of controlling magnetic hardness and reversal sharpness in FePt-L10 systems. The main findings on loops characteristics, regarding the coercive field Hc and remanence magnetization Mr, are summarized in the following table.

Table 1. Magnetic properties of L10 thin films for the various iron concentrations.

Fe (%)	A (pJ/m)	Hc (mT)	Mr (normalized)
48	10	56	0.40
60	12	66	0.44
68	13	69	0.45

The above analysis confirms that both film thickness and exchange stiffness (Fe concentration) critically determine the reversal mechanism and coercive behavior of FePt-based thin films. When the structural dimensions exceed the exchange length, the magnetization reversal transitions from localized, jump-like switching to collective domain-wall motion, resulting in smoother loops and reduced coercivity. These results establish a direct link between the simulated hysteresis features and the intrinsic micromagnetic length scales governing the behavior of exchange-coupled magnets.

 doi:10.20944/preprints202511.1187.v1

5. Conclusions

Micromagnetic simulations were carried out to investigate the magnetic behavior of $L1_0$ FePt monolayers and FePt/Fe bilayer thin films. The analysis of the FePt monolayer revealed a strong dependence of coercivity on film thickness. As the thickness increased from 1 to 10 nm, the coercivity rose markedly, reaching a maximum at 10 nm, before decreasing again at 20 nm. This non-monotonic evolution reflects a transition in the magnetization reversal mechanism: thin films below the exchange length exhibit localized switching with lower coercivity, while thicker films above this scale reverse collectively through domain-wall motion, leading to smoother loops and reduced coercivity. Variations in Fe concentration, modeled through the exchange stiffness constant, further confirmed that higher Fe content enhances magnetic rigidity and coercivity, whereas lower Fe fractions promote easier reversal and complete saturation.

Building on these results, FePt/Fe bilayer systems were simulated using the optimal FePt thickness of 2 nm, combined with Fe layers of 10 nm and 12 nm. In both cases, the bilayers exhibited rectangular, narrow hysteresis loops and full saturation at the applied field of 500 mT, confirming efficient exchange coupling between the hard (FePt) and soft (Fe) layers. The results indicate that reducing the FePt thickness transforms the system from a rigid magnet into an exchange-spring configuration, where the soft Fe layer assists the magnetization reversal of the hard FePt phase. Out-of-plane simulations of the 2 nm FePt/10 nm Fe bilayer further demonstrated a non-rectangular loop with higher coercivity and lower squareness, consistent with strong perpendicular uniaxial anisotropy arising from the FePt layer.

Consequently, the study establishes that a 2 nm FePt layer provides an optimal balance between saturation, coercivity, and stability, making it the most suitable configuration for designing exchange-spring-type FePt/Fe thin films. These findings contribute to a better understanding of thickness- and composition-dependent micromagnetic behavior in FePt-based nanostructures and can guide the optimization of high-performance magnetic materials for data storage and spintronic applications.

Author Contributions: Conceptualization, N.M. and E.P.; methodology, N.M. and E.P.; software, N.M.; validation, N.M. and E.P.; formal analysis, N.M. and E.P.; investigation, N.M. and E.P.; data curation, N.M. and E.P.; writing—original draft preparation, N.M. and E.P.; writing—review and editing, N.M. and E.P.; visualization, N.M. and E.P.; supervision, N.M. and E.P.; project administration, N.M. and E.P.; All authors have read and agreed to the published version of the manuscript.

Funding: This research received no external funding

Institutional Review Board Statement: Not applicable, this study does not involve humans or animals.

Data Availability Statement: The data presented in this study are available by the authors on request.

Conflicts of Interest: The authors declare no conflicts of interest

References

1. Ma, B.; Wang, H.; Zhao, H.; Sun, C.; Acharya, R.; Wang, J.-P. Structural and magnetic properties of a core–shell type $L1_0$ FePt/Fe exchange-coupled nanocomposite with tilted easy axis. *J. Appl. Phys.* **2011**, *109*, 083907.Author 1, A.; Author 2, B. Title of the chapter. In *Book Title*, 2nd ed.; Editor 1, A., Editor 2, B., Eds.; Publisher: Publisher Location, Country, 2007; Volume 3, pp. 154–196.
2. Weller, D.; Mosendz, O.; Parker, G.; Pisana, S.; Santos, T.S. $L1_0$ FePtX–Y media for heat-assisted magnetic recording. *Phys. Status Solidi A* **2013**, *210*, 1245–1260.
3. Weller, D.; Parker, G.; Mosendz, O.; Lyberatos, A.; Mitin, D.; Safonova, N.Y.; Albrecht, M. Review article: FePt heat-assisted magnetic recording media. *J. Vac. Sci. Technol. B* **2016**, *34*, 060801.
4. Simizu, S.; Obermyer, R.T.; Zande, B.; Chandhok, V.K.; Margolin, A.; Sankar, S.G. Exchange coupling in FePt permanent magnets. *J. Appl. Phys.* **2003**, *93*, 8134–8136.
5. Liu, L.; Sheng, W.; Bai, J.; Cao, J.; Lou, Y.; Wang, Y.; Wei, F.; Lu, J. Magnetic properties and magnetization reversal process of $L1_0$ FePt/Fe bilayer magnetic thin films. *Appl. Surf. Sci.* **2012**, *258*, 8124–8127.

 doi:10.20944/preprints202511.1187.v1

6. Xu, Z.; Zhou, S.M.; Ge, J.J.; Du, J.; Sun, L. Magnetization reversal mechanism of perpendicularly exchange-coupled composite bilayers. *J. Appl. Phys.* **2009**, *105*, 123903.
7. Makarov, D.; Lee, J.; Brombacher, C.; Schubert, C.; Fuger, M.; Suess, D.; Fidler, J.; Albrecht, M. Perpendicular FePt-based exchange-coupled composite media. *Appl. Phys. Lett.* **2010**, *96*, 062501.
8. Baldasseroni, C.; Bordel, C.; Gray, A.X.; Kaiser, A.M.; Kronast, F.; Herrero-Albillos, J.; Schneider, C.M.; Fadley, C.S.; Hellman, F. Temperature-driven nucleation of ferromagnetic domains in FeRh thin films. *Appl. Phys. Lett.* **2012**, *100*, 262401.
9. Granitzka, P.W.; Jal, E.; Le Guyader, O.; Savoini, M.; Higley, D.J.; Liu, T.; Chen, Z.; Chase, T.; Ohldag, H.; Dakovski, G.L.; et al. Magnetic switching in granular FePt layers promoted by near-field laser enhancement. *Nano Lett.* **2017**, *17*, 2426–2432
10. Victora, R.H.; Shen, X. Exchange coupled composite media for perpendicular magnetic recording. *IEEE Trans. Magn.* **2005**, *41*, 2828.
11. Makarov, D.; Lee, J.; Brombacher, C.; Schubert, C.; Fuger, M.; Suess, D.; Fidler, J.; Albrecht, M. Perpendicular FePt-based composite media. *Appl. Phys. Lett.* **2010**, *96*, 062501.
12. Liu, L.; Sheng, W.; Bai, J.; Cao, J.; Lou, Y.; Wang, Y.; Wei, F.; Lu, J. Magnetic properties and magnetization reversal process of $L1_0$ FePt/Fe bilayer magnetic thin films. *Appl. Surf. Sci.* **2012**, *258*, 8124–8127.
13. Lethole, N.; Ngoepe, P.; Chauke, H. Compositional dependence of magnetocrystalline anisotropy, magnetic moments, and energetic and electronic properties on Fe–Pt alloys. *Materials* **2022**, *15*, 5679.
14. Kehagias, T.; Karfaridis, D.; Ballani, C.; Mihalceanu, L.; Hauser, C.; Vasileiadis, I.G.; Dimitrakopulos, G.P.; Vourlias, G.; Papaioannou, E.Th. Magnetization reversal and dynamics in epitaxial Fe/Pt spintronic bilayers stimulated by interfacial Fe_3O_4 nanoparticles. *Materials* **2021**, *14*, 4354.
15. Keller, S.; Mihalceanu, L.; Schweizer, M.R.; Lang, P.; Heinz, B.; Geilen, M.; Brächer, T.; Pirro, P.; Meyer, T.; Conca, A.; et al. Determination of the spin Hall angle in single-crystalline Pt films from spin pumping experiments. *New J. Phys.* **2018**, *20*, 053002.
16. Karfaridis, D.; Mihalceanu, L.; Keller, S.; Simeonidis, K.; Dimitrakopulos, G.P.; Kehagias, T.; Papaioannou, E.Th.; Vourlias, G. Influence of the Pt thickness on the structural and magnetic properties of epitaxial Fe/Pt bilayers. *Thin Solid Films* **2020**, *694*, 137716.
17. Sakuma, A. Evaluation of the exchange stiffness constants of itinerant magnets at finite temperatures from first-principles calculations. *J. Phys. Soc. Jpn.* **2024**, *93*, 054705.
18. Ma, B.; Wang, H.; Zhao, H.; Sun, C.; Acharya, R.; Wang, J.P. $L1_0$ FePt/Fe exchange coupled composite structure on MgO substrates. *IEEE Trans. Magn.* **2010**, *46*, 2345–2348.
19. Casoli, F.; Albertini, F.; Nasi, L.; Fabbrici, S.; Cabassi, R.; Bolzoni, F.; Bocchi, C. Strong coercivity reduction in perpendicular FePt/Fe bilayers due to hard/soft coupling. *Appl. Phys. Lett.* **2008**, *92*, 142506.
20. Lakshmanan, M. The fascinating world of the Landau–Lifshitz–Gilbert equation: an overview. *Philos. Trans. R. Soc. A Math. Phys. Eng. Sci.* **2011**, *369*, 1280–1300.
21. Donahue, M.J.; Porter, D.G. *OOMMF User's Guide*, Release 1.2a; NIST: Gaithersburg, MD, USA, 2002. Available online: http://math.nist.gov/oommf/ (accessed on 30 October 2002).
22. Ghidini, G.; Asti, G.; Pellicelli, R.; Pernechele, C.; Solzi, M. Magnetic properties of Fe-based thin films. *J. Magn. Magn. Mater.* **2007**, *316*, 159.
23. Zhang, J.; Liu, Y.; Wang, F.; Zhang, J.; Zhang, R.; Wang, Z.; Xu, X. Magnetic and structural properties of FePt films. *J. Appl. Phys.* **2012**, *111*, 073910.
24. Scheuer, L.; Ruhwedel, M.; Karfaridis, D.; Vasileiadis, I.G.; Sokoluk, D.; Torosyan, G.; Vourlias, G.; Dimitrakopoulos, G.P.; Rahm, M.; Hillebrands, B.; et al. THz emission from Fe/Pt spintronic emitters with $L1_0$-FePt alloyed interface. *iScience* **2022**, *25*, 104319.
25. Abo, G.S.; Hong, Y.K.; Park, J.; Lee, J.; Lee, W.; Choi, B.C. Definition of magnetic exchange length. *IEEE Trans. Magn.* **2013**, *49*, 4937–4939.
26. Herzer, G. Anisotropies in soft magnetic nanocrystalline alloys. *J. Magn. Magn. Mater.* **2005**, *294*, 99.
27. Kipgen, L.; Fulara, H.; Raju, M.; Chaudhary, S. In-plane magnetic anisotropy and coercive field dependence upon thickness of CoFeB. *J. Magn. Magn. Mater.* **2012**, *324*, 3118–3121.
28. Antoniak, C.; Lindner, J.; Fauth, K.; Thiele, J.-U.; Minár, J.; Mankovsky, S.; Ebert, H.; Wende, H.; Farle, M. Composition dependence of exchange stiffness in Fe_xPt_{1-x} alloys. *Phys. Rev. B* **2010**, *82*, 064403.

 doi:10.20944/preprints202511.1187.v1

29. Blachowicz, T.; Ehrmann, A. Exchange bias in thin films—An update. *Coatings* **2021**, *11*, 122. https://doi.org/10.3390/coatings11020122
30. Perzanowski, M.; Zarzycki, A.; Gregor-Pawlowski, J.; Marszalek, M. Structural and magnetic properties of FePt thin films. *ACS Appl. Mater. Interfaces* **2020**, *12*, 39926–39934.
31. Yu, J.; Xiao, T.; Wang, X.; Zhou, X.; Wang, X.; Peng, L.; Zhao, Y.; Wang, J.; Chen, J.; Yin, H.; et al. A controllability investigation of magnetic properties for FePt alloy nanocomposite thin films. *Nanomaterials* **2019**, *9*, 53. https://doi.org/10.3390/nano9010053
32. Tsai, J.-L.; Sun, C.-Y.; Lin, J.-H.; Huang, Y.-Y.; Tsai, H.-T. Magnetic properties and microstructure of FePt(BN, X, C) (X = Ag, Re) films. *Nanomaterials* **2023**, *13*, 539. https://doi.org/10.3390/nano13030539